

See discussions, stats, and author profiles for this publication at: <https://www.researchgate.net/publication/231268647>

Photoelectron Imaging as a Quantum Chemistry Visualization Tool

ARTICLE *in* JOURNAL OF CHEMICAL EDUCATION · AUGUST 2011

Impact Factor: 1.11 · DOI: 10.1021/ed100177h

CITATIONS

6

READS

27

4 AUTHORS, INCLUDING:



Kostyantyn Pichugin

University of Waterloo

22 PUBLICATIONS 196 CITATIONS

SEE PROFILE



Andrei Sanov

The University of Arizona

103 PUBLICATIONS 1,450 CITATIONS


SEE PROFILE

Photoelectron Imaging as a Quantum Chemistry Visualization Tool

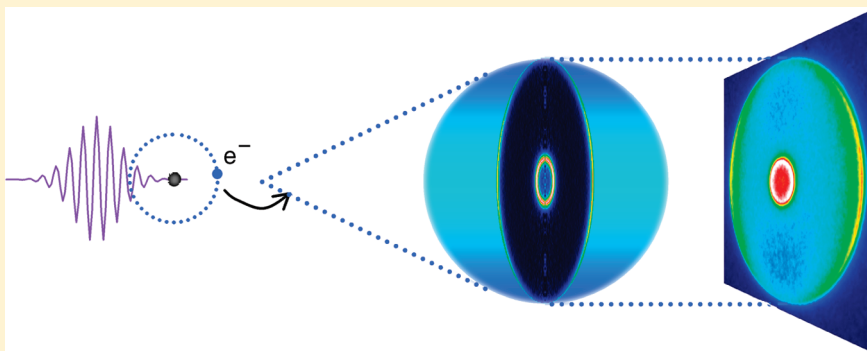
Emily R. Grumbling,[†] Kostyantyn Pichugin,^{†,‡} Richard Mabbs,[‡] and Andrei Sanov^{*,†}

[†]Department of Chemistry and Biochemistry, University of Arizona, Tucson, Arizona 85721, United States

[‡]Department of Chemistry, Washington University, Saint Louis, Missouri 63130, United States

 Supporting Information

ABSTRACT:



An overview and simple example of photoelectron imaging is presented, highlighting its efficacy as a pedagogical tool for visualizing quantum phenomena. Specifically, photoelectron imaging of H^- (the simplest negative ion) is used to demonstrate several quantum mechanical principles. This example could be incorporated into an introductory quantum chemistry course to extend the traditional discussion of the photoelectric effect and photoelectron spectroscopy into the area of matter waves. In working through this example, several core quantum-mechanical topics and concepts have been explored, such as conservation of angular momentum, the transition dipole moment, components of the hydrogenic orbitals, the Born interpretation of the wave function, and the theory of quantum measurement.

KEYWORDS: Upper-Division Undergraduate, Physical Chemistry, Analogies/Transfer, Atomic Properties/Structure, Atomic Spectroscopy, Lasers, Quantum Chemistry, Spectroscopy

Quantum chemistry is a daunting subject to many undergraduate students, in part because the underlying principles and concepts can be abstract and difficult to relate to. It has been proposed that modern experimental examples can help to ground quantum theory in clearly observable phenomena and thus facilitate learning.¹ The emerging technique of photoelectron imaging can supply such examples. A pedagogical introduction to the technique is provided, aimed at chemical educators and undergraduate students studying physical chemistry. The goal is to provide a contemporary, phenomenological means for connecting concepts in quantum theory to experimental results. Some cases where photoelectron imaging might offer a valuable, alternative illustration of key ideas are highlighted. This approach will also raise awareness of this increasingly important experimental technique in a wider audience.

INTRODUCTION TO PHOTOELECTRON IMAGING

The photoelectric effect is usually discussed in physical chemistry courses as part of the introduction to wave–particle duality and the quantization of light. This phenomenon of electron release upon irradiation of a metal surface has characteristics that cannot be explained by classical physics. First,

increasing the light's intensity increases the number of electrons released, contrary to the classical expectation that it should increase the speed with which they depart. On the other hand, increasing the frequency of the radiation does increase the speed (or kinetic energy) with which the electrons are ejected, and the classical expectation that there should be an increase in the number of electrons released is not realized! Finally, decreasing the frequency to a certain point (unique to the type of metal) causes the electron emission to cease, regardless of the light's intensity.

These observations necessitate a description of light as having both particle- and wave-like attributes. Light is indivisible beyond discrete packets, now called photons,² each with energy defined by the light's frequency. The photoelectric effect was explained by Albert Einstein in one of the papers² of his *annus mirabilis*, as a one-photon, one-electron process where part of the photon's energy is spent in overcoming the binding force, with the excess converted into kinetic energy of the released electron (or "photoelectron"). For photons whose energy is above the cutoff frequency, electrons may be liberated with kinetic energy (eKE)

Published: August 05, 2011

of

$$eKE \leq h\nu - \Phi \quad (1)$$

where Φ , the work function of the metal, is the smallest photon energy for which photoemission may occur. The photoelectric effect is the most commonly used classroom example of the quantization of light energy.

Applying the light source to atoms and molecules also reveals quantized energy levels in matter. Photoelectron spectroscopy has become an extremely useful and versatile tool for probing the energies of atomic and molecular orbitals.³ This is usually done through interpretation of the photoelectron energy spectrum, which indicates the probability of the emitted electrons having a certain kinetic energy. The photoelectron spectrum contains the probability of removal of an electron from a given orbital and the amount of energy required to do so, often yielding information about the energy spacing of electronic and vibrational levels in atoms and molecules.

It is less appreciated that photoelectrons produced using polarized radiation have characteristic distributions of the *directions* of their velocities. These distributions, referred to as photoelectron angular distributions, are generally anisotropic. This arises due to the quantization of angular momentum. Students of chemistry generally appreciate that atomic orbitals have defined shapes and symmetries based upon their orbital angular momentum. Similarly, the angular distribution of the photoelectrons is dependent on angular momentum, related through selection rules to the shape of the orbital from which it was removed. In particular, interpretation of photoelectron angular distributions for isolated atomic or molecular systems yields insight into the structure and symmetry of the parent orbitals from which the electrons were ejected.

Photoelectron imaging combines photoelectron spectroscopy with a photographic approach to quantify photoelectron distributions upon detachment from gas-phase chemical systems. This elegant experimental technique probes both electronic energy eigenvalues and the properties of the corresponding wave functions. Research groups apply photoelectron imaging to negative ions. The term “photodetachment” refers to the process of removing an electron from an anionic species to leave a neutral molecule or atom behind. Photodetachment generally requires significantly less energy than photoionization (removal of an electron from a neutral molecule), allowing the use of visible rather than extreme ultraviolet or X-ray photons.

Technical details of the instrumentation are described elsewhere.⁴ In brief, negative ions formed in a high-vacuum environment are separated according to their mass-to-charge ratios using a pulsed time-of-flight mass spectrometer. A pulsed laser beam is timed to irradiate only the ions of interest, resulting in a few photodetachment events each experimental cycle. A static electric field generated by a set of velocity-map imaging electrodes (Figure 1) has the effect of (i) projecting the photoelectrons onto a two-dimensional, position-sensitive detector; (ii) focusing (or “flattening”) the photoelectron distribution longitudinally onto the plane of the detector; and (iii) mapping all identical photoelectron velocity components onto the same position on the detector regardless of the exact position from which the photoelectron originated in the laser-ion interaction region. The images resulting from accumulation of $\sim 10^5$ individual electron impacts represent the probability distribution of the photoelectrons in the plane of the detector, reflecting both

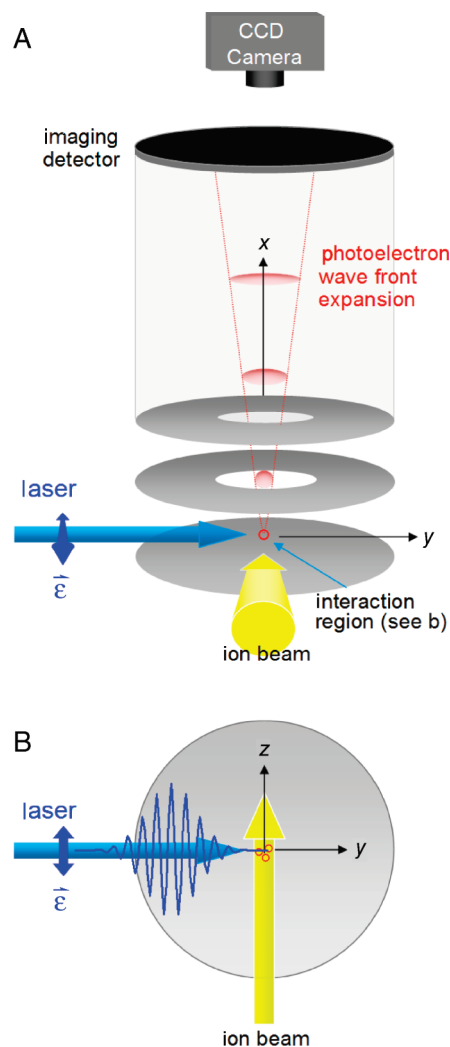


Figure 1. (A) Side view of the photoelectron imaging assembly. The three circular electrodes comprising the velocity-map imaging lens are shown in gray. The laser's electric field vector, \vec{E} , is parallel to the plane of the detector and indicated by the blue double-headed arrow (directed perpendicular to the plane of the page). The photoelectron wavefront (red) is projected onto the detector along the x axis. (B) Top view of the laser-ion interaction region. The laser beam (blue) propagates in the y direction; \vec{E} lies along the z axis, parallel to the ion beam (yellow). The electrodes and detector are parallel to the yz plane.

the traditional photoelectron energy spectrum and the photoelectron angular distribution.

The visual nature of the photoelectron image makes it an automatic object of curiosity for a student. This curiosity can be used to stimulate an interest in the information content of the image, providing a compelling new context within which to explore the principles taught to undergraduate quantum chemistry students, either in lecture or as part of a homework or classroom discussion activity. For example, faculty could examine this framework for themselves or introduce this material to their students during lecture as an alternate illustration of certain principles (such as electronic transition selection rules). Related questions could be included in homework assignments to prompt creative application of fundamental principles. More advanced students might enjoy reading this article.

The simplest negative ion, H^- , has been chosen as a tutorial system, for which some imaging results have been reported.⁵ Hydride relates directly to the quantum-mechanical Hamiltonian for the hydrogen atom, the solutions of which form the groundwork for understanding electronic structure and chemical bonding. In the following, our independent study of H^- is used as a new context for discussion of concepts that are key to quantum chemistry.

WAVE–PARTICLE DUALITY OF MATTER

Wave–particle duality is at the heart of quantum mechanics. Einstein's explanation of von Lennard's photoelectric effect measurements clearly showed that light has both particle-like and wave-like properties. Though not typically emphasized in the context of the photoelectric effect or photoelectron spectroscopy, objects with a nonzero inertial mass (which classically would be considered particles) also behave like waves. The characteristic wavelength (λ) is dependent on the particle's momentum (p) according to the de Broglie relation: $\lambda = h/p$, where h is Planck's constant.

Chemists rely upon this principle; the description of molecular structure is based upon electron wave functions that define atomic and molecular orbitals. A similar approach holds for free electrons with the key distinction that electrons in molecules are in bound, spatially localized states, whereas a free electron is a boundless, propagating wave.

When an electron is photodetached from a negative ion, its behavior should be viewed as wave-like. As the electron departs, its average separation from the remaining neutral species increases with time. However, the direction in which the electron travels is usually fundamentally undefined. A photoelectron ejected from a molecule can be thought of as a spherically expanding wavefront, similar to an inflating balloon whose surface becomes increasingly distant from its center. In photoelectron imaging, photoelectrons are probed after a set expansion time by projecting them onto the detector.

QUANTUM MEASUREMENT AND PROBABILITY DENSITIES

The interaction of the electron wavefront with the detector constitutes an act of measurement, which collapses the wave function into one of the eigenfunctions of the measurement operator. Because the eigenfunctions of the position operator are delta functions of the coordinates, measurement results in a single observable impact spot. Thus, even though quantum mechanical descriptions of electrons are cast in terms of wave functions, each individual electron is observed as impacting the detector in a single spot, which reinforces the intuitive perception of electrons as microscopic particles.

A single measurement does not reveal the inherently delocalized probability distribution associated with a photoelectron; it results in only one of the possible outcomes. However, by repeating the same experiment many times, a statistical distribution of measured impact positions is accumulated, mapping the probability density of photoelectrons. According to the Born interpretation of quantum mechanics, the distribution measured for many photoelectrons detached from identical systems reflects the square modulus of the wave function for a *single* photoelectron immediately before impacting the detector.

The experimental process of acquisition of a photoelectron image, and hence the accumulation of the photoelectron probability density distribution, can be demonstrated using either an animated

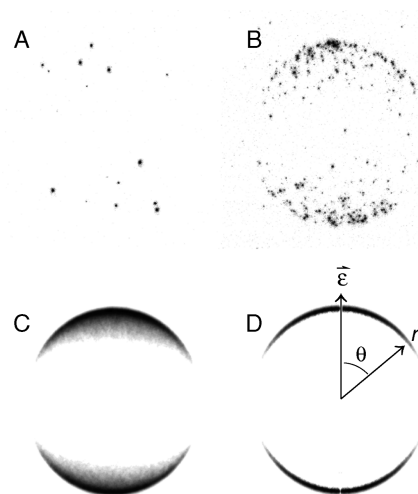


Figure 2. Recording of photoelectron impacts after detachment from H^- using 800 nm (1.55 eV) photons: (A) Electrons impact the detector as localized, seemingly random spots. Image corresponding to detection of approximately 15 photoelectrons. (B) The emerging pattern due to many (~ 200) electron impacts. (C) The noise-subtracted, intensity-scaled distribution for $\sim 200,000$ photoelectrons. Darker areas indicate a greater number of electron impacts. (D) Reconstructed cross-section of the 3D distribution. The electric field polarization vector for the laser radiation is vertical in the plane of the image.

compilation (see the Supporting Information for an animation of the accumulation process) or a sequence of selected acquisition frames. The accumulation of photoelectron impacts on the detector for 800 nm photodetachment from H^- is illustrated in Figure 2. The relatively few events in Figure 2A, resulting from a small number of experimental cycles, seem randomly distributed, but by the time as few as ~ 200 events have been accumulated (Figure 2B), a circular pattern begins to emerge. The pattern is much better defined in Figure 2C, which is the result of approximately 200,000 event measurements. The distance from any point to the image center is proportional to the electron speed in the plane of the detector.

IMAGE ANALYSIS

The photoelectron image is the projection of a 3D probability density function onto the 2D detector. However, if the laser light is linearly polarized, the original distribution is cylindrically symmetric about the polarization axis (here the z axis). Thus, the 3D distribution is actually a function of only two variables (r and z). If the z axis is parallel to the detector, the recorded image is an Abel transformation (i.e., projection) of the original cylindrically symmetric distribution. The 3D distribution is recovered via an inverse Abel transformation,⁶ which returns a slice through the center of the cylindrically symmetric photoelectron cloud (see the appendix included in the Supporting Information for description and animated illustration of Abel and inverse Abel transforms). The “Abel-inverted” slice for H^- is shown in Figure 2D. It represents the electron probability density as a function of r , the distance from the center, and θ , the angle with respect to the z axis. Rotation of this reconstructed slice about the z axis retraces the entire 3D distribution.

THE PHOTOELECTRON ENERGY SPECTRUM AND ANGULAR DISTRIBUTION

Integrating the cylindrically symmetric 3D distribution over the entire range of θ yields the photoelectron distribution as a

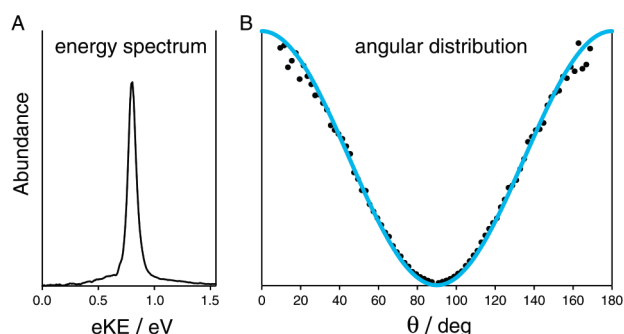


Figure 3. (A) Photoelectron spectrum for H^- with $h\nu = 1.55$ eV ($\lambda = 800$ nm). (B) Angular distributions: black circles correspond to normalized experimental photoelectron signal intensities as a function of angle. For clarity, only every 5th data point is shown. The solid blue line corresponds to the square modulus of the spherical harmonic for $l = 1$ and $m_l = 0$, $|Y_{10}|^2 \propto \cos^2 \theta$.

function of r , which is proportional to the electron speed. An appropriate coordinate transformation from r to electron kinetic energy, eKE, produces the photoelectron spectrum, shown for H^- in Figure 3A. The spectral line width is due to various instrumental factors.⁴

The spectrum in Figure 3A peaks at eKE = 0.80 eV. For $h\nu = 1.55$ eV, this corresponds to an electron binding energy eBE = $h\nu - \text{eKE} = 0.75$ eV, which is the electron affinity of atomic hydrogen. The above expression is analogous to eq 1, with the work function Φ replaced with the eBE. The imaging result thus provides an alternative demonstration of the concepts involved in the photoelectric effect and photoelectron spectrum.

In addition to the radial coordinate, the photoelectron signal intensity in Figure 2C,D also varies with respect to θ , reflecting the angular dependence of the free-electron probability density. The photoelectron angular distribution is calculated by integrating the slice in Figure 2D with respect to r and plotting the result as a function of θ , as shown in Figure 3B. In general, the angular distribution in one-photon detachment has the form:

$$I(\theta) \propto 1 + \beta(3 \cos^2 \theta - 1)/2 \quad (2)$$

where β is the unitless anisotropy parameter.⁷ The values of β may range from -1 to 2 . Positive values indicate a photoelectron angular distribution peaking in the direction parallel to the laser polarization vector (such as in Figure 2), whereas negative values indicate predominantly perpendicular photoelectron emission. By fitting eq 2 to the experimental data for H^- , as shown in Figure 3B, the value of $\beta = 1.92 \pm 0.04$ was determined, which is close to the limiting case of $\beta = 2$, corresponding to a purely parallel (cosine-squared) angular distribution.

The photoelectron angular distribution is related to the parent atomic orbital via the relevant selection rules. In the following, the selection rules are applied to the transformation of the electron from a bound $1s$ atomic orbital to an evolving photoelectron wave upon absorption of a photon:



■ CONSERVATION OF ANGULAR MOMENTUM

The physical significance is extracted from the photoelectron angular distribution $I(\theta)$ by first considering the $\Delta l = \pm 1$

selection rule for a one-photon, electric-dipole allowed transition. The absorbed photon carries one quantum of angular momentum, which is transferred to the electron upon photo-detachment. Because $l = 0$ for the $\text{H}^- 1s$ orbital, the free electron must have $l = 1$, corresponding to a “p wave”, similar to an atomic p orbital, but with a different (unbound and time dependent) radial component.

The image in Figure 2C is consistent with the photoelectron having p_z character—the image shows a single node perpendicular to the z axis, corresponding to a cosine-squared angular distribution. The bound- and free-electronic wave functions corresponding to a given value of l (and m) have the same angular dependence, differing only in the radial parts. In the case of a p_z free-electron wave, as well as for a bound p_z orbital, the angular distribution is calculated as $I(\theta) \propto |Y_{10}|^2$, where Y_{10} is the angular part of the wave function, the spherical harmonic for $l = 1$ and $m = 0$. This limiting distribution is superimposed with the experimental data in Figure 3B. In the following, the rationale as to why the free-electron p wave, in this case, is polarized along the z axis rather than the x or y axes is examined.

■ THE TRANSITION DIPOLE MOMENT

For a transition to be allowed under the one-photon and electric-dipole approximations, the transition dipole moment, defined as

$$\vec{\mu}_{fi} = \int_{\text{all space}} \psi_f^*(r, \theta, \phi) \hat{\mu} \psi_i(r, \theta, \phi) d\tau = \langle \psi_f | \hat{\mu} | \psi_i \rangle \quad (4)$$

must be nonzero. In eq 4, $\hat{\mu} = -e\vec{r}$ is the electric dipole operator, $d\tau$ is the infinitesimal volume element, while ψ_i and ψ_f are the wave functions representing the initial (bound) and final (free) states of the electron, respectively. The transition *amplitude* is proportional to the scalar product of $\vec{\mu}_{fi}$ and the electric field vector. The transition *probability* P is given by

$$P \propto |\vec{\mu}_{fi} \cdot \vec{\epsilon}|^2 = |\mu_{fi,x}\epsilon_x|^2 + |\mu_{fi,y}\epsilon_y|^2 + |\mu_{fi,z}\epsilon_z|^2 \quad (5)$$

where $\vec{\epsilon}$ is the laser light's electric field vector.

For z polarized laser light, only the z component of the transition moment is important, because $\epsilon_x = \epsilon_y = 0$. The condition for the absorption of a photon is therefore

$$\begin{aligned} \mu_{fi,z} &= -e \int_{\text{all space}} \psi_f^*(r, \theta, \phi) z \psi_i(r, \theta, \phi) d\tau \\ d\tau &= -e \langle \psi_f | z | \psi_i \rangle \neq 0 \end{aligned} \quad (6)$$

where the definition of the dipole operator is used. The integration in eq 6 is over all space. However, only the angular components of the wave functions need be considered to understand the photoelectron angular distribution. The angular part of each possible final state wave function is identical to the angular part of a hydrogenic orbital and can be expressed as a spherical harmonic function, Y_{lm} . Considering only the angular components and recalling that $d\tau = r^2 \sin \theta dr d\theta d\phi$, the

condition in eq 6 simplifies to

$$\int_0^{2\pi} \int_0^\pi Y_f^*(\theta, \phi) z Y_i(\theta, \phi) \sin \theta \, d\theta \, d\phi = \langle Y_f | z | Y_i \rangle \neq 0 \quad (7)$$

where Y_i and Y_f are the spherical harmonics corresponding to the initial (bound) and final (free) states of the electron, respectively. For photodetachment from the 1s orbital of H^- , $Y_i = Y_{00}$ and $Y_f = Y_{\ell m}$ where $\ell = 1$, so that the possible values of m are 0 and ± 1 . Because Y_{00} is an even function, whereas z is odd, the integral in eq 7 is nonzero only if Y_f^* is odd with respect to the z axis. Therefore, the only allowed free-electron wave in this case is that for which $m = 0$, corresponding to the p_z wave.

This result can be illustrated pictorially using the common visualizations of the real p_x , p_y , and p_z angular functions instead of those for p_0 and $p_{\pm 1}$:

$$\left\langle \begin{array}{c} \text{free } p_x \\ \text{wave} \end{array} \middle| \hat{z} \middle| \begin{array}{c} \text{bound } 1s \\ \text{orbital} \end{array} \right\rangle = 0 \quad (8)$$

$$\left\langle \begin{array}{c} \text{free } p_y \\ \text{wave} \end{array} \middle| \hat{z} \middle| \begin{array}{c} \text{bound } 1s \\ \text{orbital} \end{array} \right\rangle = 0 \quad (9)$$

$$\left\langle \begin{array}{c} \text{free } p_z \\ \text{wave} \end{array} \middle| \hat{z} \middle| \begin{array}{c} \text{bound } 1s \\ \text{orbital} \end{array} \right\rangle \neq 0 \quad (10)$$

These illustrations confirm that the only final state that corresponds to a nonzero value of the z component of the transition dipole moment for photodetachment from the bound 1s orbital is the free p_z ($\ell = 1, m = 0$) wave. Thus, the only free-electron waves allowed in the one-photon, one-electron photodetachment of H^- ($1s^2$) using linearly z polarized light are p_z waves, with intensity peaking in the laser polarization direction (at 0° and 180°). This prediction is in agreement with the experimental angular distribution seen in Figures 2B–D and 3B. It is worth noting that the three-dimensional distribution will be p -like with respect to the laser polarization axis, regardless of the laboratory-frame configuration. However, in the event that the polarization is perpendicular to plane of the detector, that is, along the x axis indicated in Figure 1A, the cylindrical symmetry about this axis would result in a seemingly isotropic photoelectron image and necessitate a different image reconstruction technique to obtain the original 3D distribution.

■ EXTENSION TO OTHER ANIONS

Using H^- as an example, the photoelectron angular distribution is shown to be related through symmetry to the wave function of its initial state. It is noteworthy that the results for H^- are qualitatively consistent with the classical expectations. The interaction of the oscillating electric field of light (described as classical electromagnetic wave) with bound electrons (described as particles or a charged cloud) would result in an external force parallel to the electric field vector and should therefore eject electrons predominantly along the laser polarization axis. This classical prediction is in qualitative agreement with

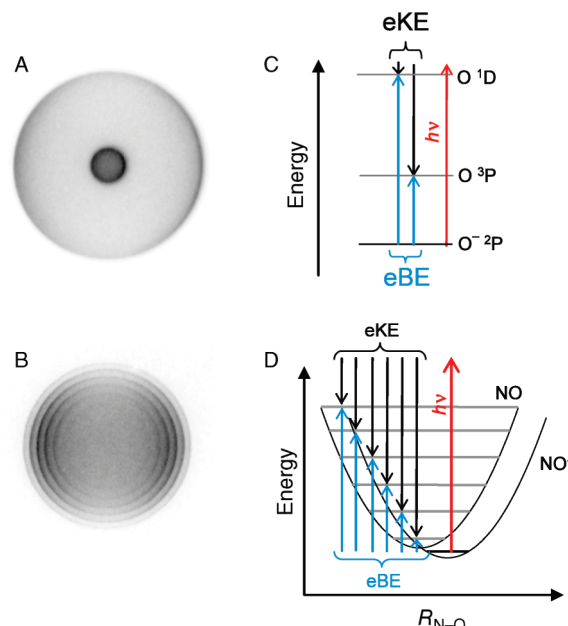


Figure 4. Photoelectron images for detachment from (A) O^- at 355 nm and (B) NO^- at 785 nm (images are not to scale). The multiple transitions in each image correspond to generation of multiple (A) electronic or (B) vibrational states of the remaining neutral species. The final state energy levels are indicated in C (electronic, for O^-) and D (vibrational, for NO^-).

the photoelectron angular distribution observed for H^- (Figure 2). However, classical theory generally fails to predict the nature of photoelectron angular distributions; in many photoelectron images the intensity peaks in the direction perpendicular to the light's electric field vector.

Two such examples, arising from photodetachment of electrons from (i) a $2p$ atomic orbital of O^- and (ii) the π^*2p molecular orbital of NO^- , are illustrated in Figure 4. In both cases, the photodetachment intensity reaches a maximum in the direction perpendicular to the laser polarization axis, an effect that can be explained only within the quantum-mechanical framework. The multiple rings in each image correspond to generation of different electronic or vibrational states of the remaining neutral species, respectively. The energy-level diagrams (Figure 4C,D) indicate the energetically accessible final states of the neutral species for each case. Within the energy resolution of the experiment, there is one radial band for each neutral state.

For atomic orbitals with $\ell_i > 0$, conservation of angular momentum allows for two possible types of outgoing waves ($\ell_f = \ell_i \pm 1$), each containing its own radial and angular components. The photoelectron wave functions in such cases are coherent superpositions of both allowed wave types. The relative contributions of each "partial" wave are dependent upon the kinetic energy of the photoelectron. This leads to energy dependence of the photoelectron angular distributions.

Photoelectron angular distributions for photodetachment from molecular anions are even more complicated, in part due to the lack of well-defined angular-momentum quantum numbers for molecular species. However, general symmetry arguments may still be used, with considerable success, to shed light on the properties of the parent molecular orbitals. Interested readers are referred to ref 8 for further discussion of angular distributions in atomic and molecular-anion photodetachment.

CONCLUSIONS

Photoelectron imaging combines traditional photoelectron spectroscopy with “photography” of quantum objects, yielding snapshots of photoelectron probability densities. This provides a layered approach to the quantum nature of chemical systems: by probing both a system’s quantum energy levels and the properties of its wave functions. The unique visual accessibility of imaging makes it a potentially effective teaching tool.

We have built a tutorial example of the pedagogical value of photoelectron imaging using a straightforward experimental result for H^- . This example (as well as others) could be easily incorporated into an introductory quantum chemistry course to extend the traditional discussion of the photoelectric effect and photoelectron spectroscopy into the area of matter waves. In working through this example, several core quantum-mechanical topics and concepts have been explored, such as conservation of angular momentum, the transition dipole moment, components of the hydrogenic orbitals, the Born interpretation of the wave function, and the theory of quantum measurement. It is hoped that this work provides a valuable perspective on experimental quantum mechanics that will encourage further exposure of undergraduates to contemporary research in physical chemistry.

ASSOCIATED CONTENT

Supporting Information

Appendix; the first animation (Quicktime format) demonstrates accumulation of photoelectron signal as recorded by our detector, with each frame corresponding to one second of exposure. Each individual impact point corresponds to detection of an electron (some due to noise). At first, the impact points appear random. However, upon accumulation of these impacts, a clear pattern emerges, corresponding to the probability density of any single photoelectron immediately before detection. Background is collected separately for subtraction from the final image (not pictured); the second animation (Moving Picture Experts Group format) illustrates the process of Abel Inversion for the model spherical-shell distribution described in the Appendix. This material is available via the Internet at <http://pubs.acs.org>.

AUTHOR INFORMATION

Corresponding Author

*E-mail: sanov@u.arizona.edu.

Present Addresses

*Max Planck Research Department for Structural Dynamics, University of Hamburg, Center for Free Electron Laser Science, DESY, D-22607 Hamburg, Germany.

ACKNOWLEDGMENT

The authors would like to thank Simeen Sattar (Bard College) and Vicente Talanquer (The University of Arizona) for their feedback on this writing. We also thank Amy Grumbling for animation assistance with some of the Supporting Information. Funding for this work was provided by the U.S. National Science Foundation through grants CHE-0713880 and CHE-1011895 (The University of Arizona) and CHE-0748738 (Washington University).

ADDITIONAL NOTE

^a The term “photon” was coined by G. N. Lewis in 1926.

REFERENCES

- (1) Ellison, M. D. The particle inside a ring: A two-dimensional quantum problem visualized by scanning tunneling microscopy. *J. Chem. Educ.* **2008**, *85* (9), 1282–1287.
- (2) (a) Einstein, A. Über einen die Erzeugung und Verwandlung des Lichtes betreffenden heuristischen Gesichtspunkt. *Ann. Phys.* **1905**, *17*, 132–148. (b) English translation: On a heuristic point of view about the creation and conversion of light. In *The Old Quantum Theory*; ter Haar, D., Ed.; Pergamon Press: Oxford, 1967; pp 91–107.
- (3) Sanov, A.; Mabbs, R. Photoelectron imaging of negative ions. *Int. Rev. Phys. Chem.* **2008**, *27* (1), 53–85.
- (4) Surber, E.; Mabbs, R.; Sanov, A. Probing the electronic structure of small molecular anions by photoelectron imaging. *J. Phys. Chem. A* **2003**, *107*, 8215–8224.
- (5) Reichle, R.; Helm, H.; Kiyani, I. Y. Photodetachment of H^- in a strong infrared laser field. *Phys. Rev. Lett.* **2001**, *87*, 243001.
- (6) Heck, A. J. R.; Chandler, D. W. Imaging Techniques For the Study of Chemical-Reaction Dynamics. *Annu. Rev. Phys. Chem.* **1995**, *46* (1995), 335–372.
- (7) (a) Cooper, J.; Zare, R. N. Angular Distributions in Atomic Anion Photodetachment. *J. Chem. Phys.* **1968**, *48*, 942–943. (b) Cooper, J.; Zare, R. N. Angular Distributions in Atomic Anion Photodetachment (Erratum). *J. Chem. Phys.* **1968**, *49*, 4252.
- (8) Mabbs, R.; Grumbling, E. R.; Pichugin, K.; Sanov, A. Photoelectron Imaging: A window into electronic structure. *Chem. Soc. Rev.* **2009**, *38*, 2169–2177.